

# Plucking a liquid chord: mechanical response of a liquid crystal filament

Ralf Stannarius, Alexandru Nemeş, and Alexey Eremin  
University of Magdeburg, Institute of Experimental Physics,  
Universitätsplatz 2, D-39106 Magdeburg, Germany  
e-mail: ralf@stannarius.de

## Abstract

*This paper describes an investigation of mechanical properties of freely suspended liquid filaments. These unique fluid microstructures may be formed by layered liquid crystalline mesophases. The filaments are electrically deflected and stimulated to mechanical oscillations. Resonance frequencies and damping rates are recorded. We introduce a model for a basic description of the dynamics, which is used to evaluate and to discuss the forces involved. The dependence of the oscillation parameters upon geometrical parameters and temperature is analyzed.*

Thin liquid fibers are among the most fascinating structures in complex fluids. In some non-Newtonian liquids, fibers can form in rheological processes when such material is pulled from a reservoir, for example in polymer nematics and columnar phases [1, 2]. Nematic ordering also plays a role in biological filaments, e.g. [3]. In this study, we investigate filaments that are not stabilized by dynamic effects but primarily by their internal molecular layer structure. It is well known that smectic liquid crystals, similar to soap solutions, can form thin stable free standing films. Few phases of bent-core mesogens, however, are known to form freely suspended filaments, for example when the material is pulled with a needle from the bulk. Only few investigations have been devoted so far to the understanding of structural and mechanical properties of such filaments [6, 5, 7, 4], and little is known about dynamical properties of such structures. The filaments are excellent models study fluid dynamics in microsystems.

The filamental structures represent either single cylindrical fibrils or bundles of fibrils, with diameters from fractions of micrometers to approximately 100  $\mu\text{m}$ , and slenderness ratios (length to diameter) exceeding 1000. Filaments are pulled with a needle at moderate speed ( $< 1$  mm/s) from bulk material. They retain uniform diameters during the pulling process, new material is constantly supplied from the meniscus. When the needle is pushed slowly back towards the support, the filaments remain straight and excess material flows back into the bulk. Only after a sudden fast retrace of the needle, the filaments deflect for a moment before they straighten again, on a millisecond time scale.

The aim of this study is the understanding of the dynamical properties of such liquid "chords". For that purpose, we deflect filaments of 10 to 60  $\mu\text{m}$  diameter and 1.5 mm

length laterally by means of electric fields (Fig. 1, top). After the field is switched off, the relaxation dynamics of the filaments is investigated. We observe damped oscillations of a spatially sinusoidal ground mode and analyze the dependence of oscillation parameters upon filament dimensions and temperature.

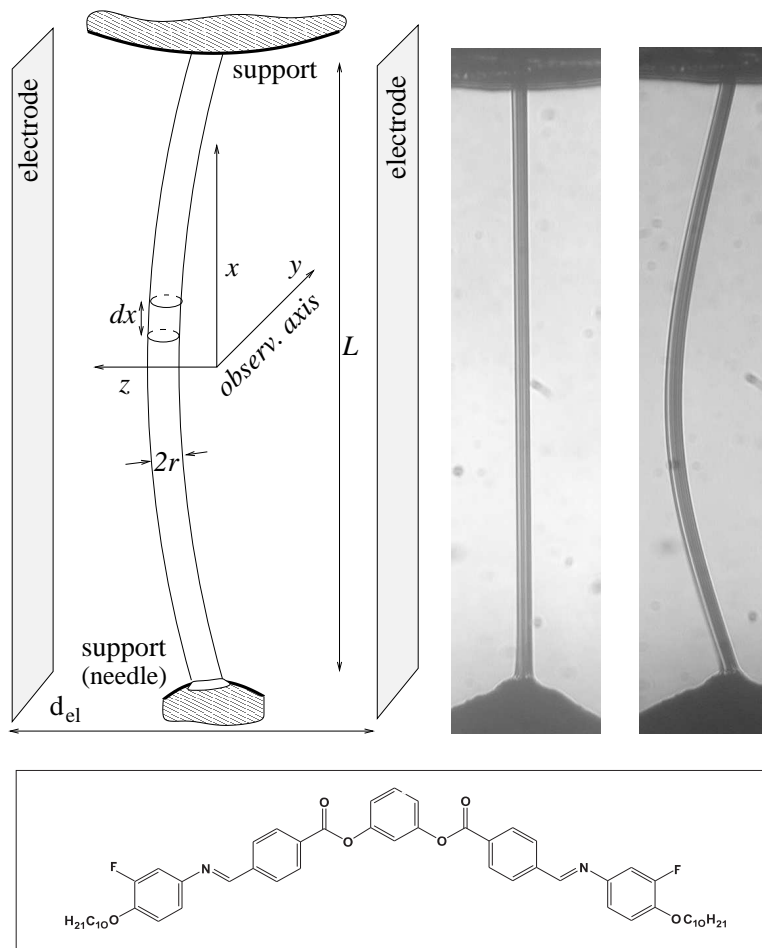


Figure 1: **Top: Experimental setup for the preparation of liquid filaments and excitation of oscillations.** The observation direction is  $y$ , the direction of the electric field and of the oscillations is  $z$ , and  $x$  is the vertical axis of the straight filament. The gap between the electrodes is 6 mm. **On the right, images of a straight (0 MV/m) and a deflected filament (0.5 MV/m) are shown, the filament length is 5.0 mm.** **Bottom: Chemical structure of the mesogen**

The material studied (Fig. 1, bottom) has a mesomorphism iso  $160^\circ\text{C SmX}$   $143^\circ\text{C SmCP}_A$   $90^\circ\text{C}$  solid. The so far not fully classified  $\text{SmX}$  phase has a layer structure and many features in common with a  $B_7$  phase [8]. X-ray data indicate that the filaments consist of cylindrically wrapped molecular layers [4], in accordance with proposed  $B_7$  filament structures [5, 6]. However, reflexes related to any in-plane molecular lattice are absent in  $\text{SmX}$ .

The experimental setup is sketched in Fig. 1. The filament is drawn vertically between two holders (positions  $x = \pm L/2$ ). Their distance can be controlled by a stepper motor.

We assume that the filaments have roughly cylindrical shape with radius  $r$ . The setup is enclosed in a custom-made heating box, described elsewhere [9]. With a homogeneous DC electric field perpendicular to the filament axis, the chord is "plucked", a well defined bend deformation is induced (Fig. 1, top right), consisting essentially of the ground mode  $z(x) = z_0 \cos(kx)$  with  $k = \pi/L$ . The deflection amplitude  $z_0$  depends on filament length and diameter and on the electric field strength. The latter is chosen between  $\approx 0.1$  and  $0.5$  MV/m, so that  $z_0$  is a few percent of the filament length.

We record the filament dynamics at frame rates up to 5/ms with a high speed camera (Citius Imaging C10), mounted on a QM 100 long range microscope. The deflection  $z$  is measured with a resolution of  $\approx 1 \mu\text{m}$  at the antinode of the oscillations,  $x = 0$ .

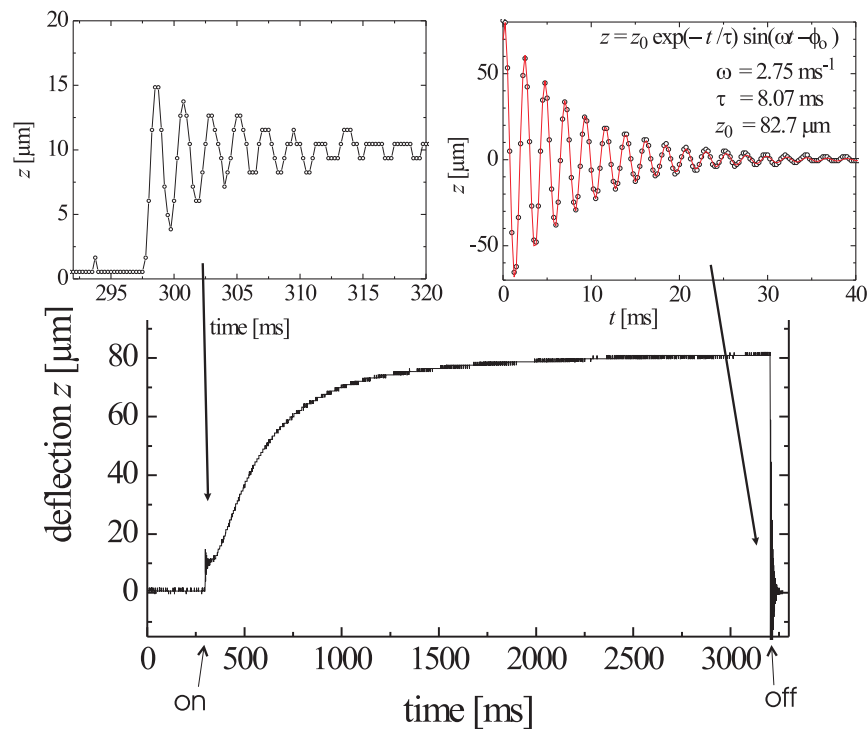
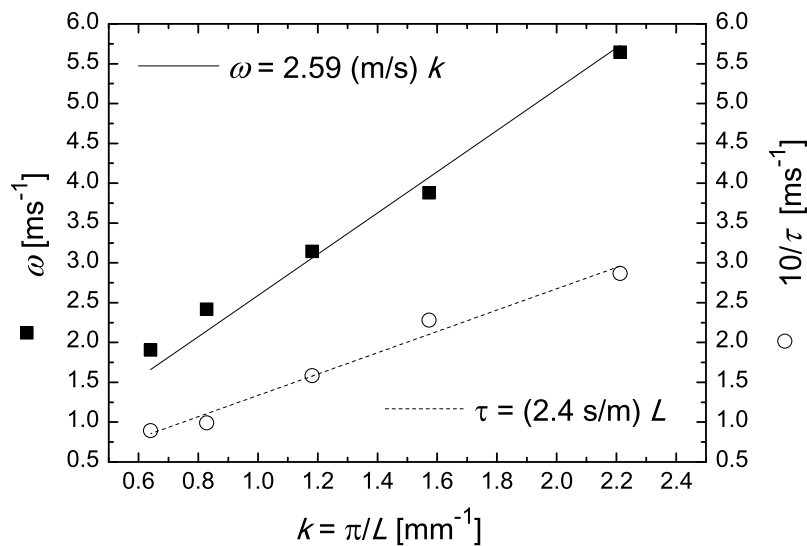


Figure 2: Deflection of a filament ( $L = 2.96$  mm,  $r = 25 \mu\text{m}$ ) at  $150^\circ\text{C}$  after switching an electric field of  $E = 0.33$  MV/m on after  $0.297$  s and off after  $3.20$  s. The left insert expands the oscillations immediately after switching on, the solid line guides the eye. The right insert shows the free oscillation after switching off, the solid curve is a fit to a damped sine curve, Eq. (1), with parameters given in the plot.

Typical experimental data are presented in Fig. 2. After the DC electric field  $E$  is switched on, the filament bends within  $\mu\text{s}$  towards one (spontaneously chosen) electrode. This deflection is induced primarily by the dielectric torques that tend to rotate a long cylinder (dielectric constant  $> 10$ ) with its axis towards the electric field axis. The deflection stops after reaching a few  $\mu\text{m}$  when a balance of electric forces and filament tension is reached, and a weak, damped oscillation follows (Fig. 2, left insert). Then, the deflected filament gradually charges in the field (flow of ionic charges of impurities), since the deflected filament is not on an equipotential line of the electric field. The charged filament is attracted

by the oppositely charged electrode, and the deflection increases until Coulomb forces acting on the filament are balanced by its tension. The charging process stops when the electric field of the accumulated charges compensates the external field in the filament. Then, the filament is again along an equipotential line of the total field. This saturation is reached after few seconds. The sign of the charge depends upon the initial spontaneous deflection, and thus the direction of bend is independent of the DC field polarity. These electric effects are essentially different from those reported for axial fields [5]. Owing to the cylindrical symmetry, there is no polar electric response. When the electric field is switched off, the filament returns with a damped oscillation to its straight ground state (right insert of Fig. 2). The frequency of this free oscillation was systematically larger, by few percent, than that of the initial vibration (left insert of Fig. 2). Since the latter may involve electric interactions additional to mechanical forces, we concentrate here only on the oscillations in the field off state.



**Figure 3: Dependence of the oscillation frequency  $\omega$  and the damping coefficient  $\tau^{-1}$  on the inverse filament length  $1/L$  at constant filament radius of  $r = 25 \mu\text{m}$ ,  $T = 150 \text{ }^\circ\text{C}$ .**

The oscillation amplitudes are fitted with a function

$$z(x=0) = z_0 \exp(-t/\tau) \cos(\omega t - \phi_0) \quad (1)$$

(see right insert of Fig. 2), the fit parameters  $\omega$  and  $\tau$  depend on temperature and filament dimensions, but neither on the electric field strength used in the preparation nor on the initial deflection amplitude.

Figure 3 shows one important experimental result,  $\omega$  depends inversely on the filament length  $L$ , i.e. the phase velocity  $c = \omega/k$  of transversal waves of the filament is constant. This representative graph shows data collected from a single filament with uniform radius, which has been drawn in five steps from 1.4 to 4.9 mm length. This length change tunes the resonance of the chord approximately from  $f = 900 \text{ Hz}$  to  $265 \text{ Hz}$ . The relaxation time  $\tau$  depends linearly upon  $L$ , but  $1/\tau$  is more than one order of magnitude smaller than  $\omega$ .

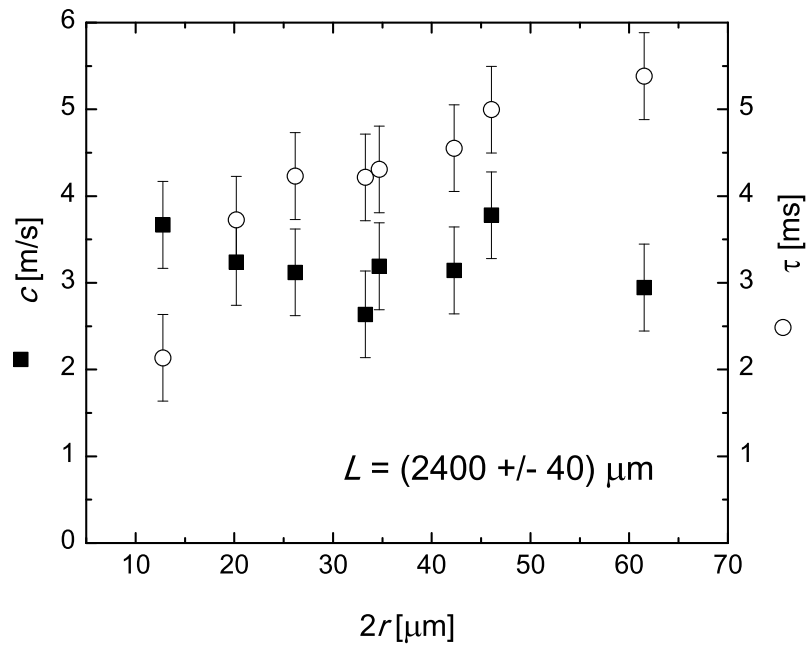


Figure 4: Dependence of the phase velocity  $c(r) = \pi\omega(r)/L$  and the damping constant  $\tau(r)$  on the filament radius  $r$ . The filament lengths are  $2.4 \text{ mm} \pm 3\%$ ,  $T = 150 \text{ }^\circ\text{C}$ .

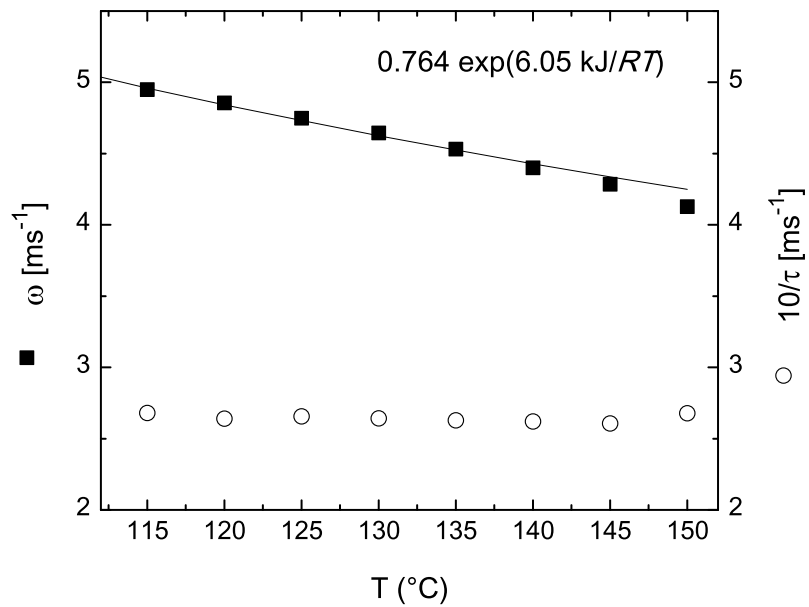


Figure 5: Dependence of the parameters  $\omega$  and  $1/\tau$  on temperature (filament diameter  $22 \mu\text{m}$ , length  $2.5 \text{ mm}$ ). The solid line is an Arrhenius fit in SmCP.

Data for the radius dependence of  $c$  and  $\tau$  (Fig. 4) scatter somewhat more than the length characteristics, because each datum point is obtained from a different filament (altogether differing in length by  $< 3\%$ ). The data do not show any systematic variation of  $\omega$  with  $r$ . The damping time decreases slightly but systematically with smaller filament radius. For a filament with a diameter of  $22\ \mu\text{m}$  and a length of  $2.5\ \text{mm}$ , we have measured the temperature dependence of both dynamic parameters. The damping time  $\tau$  is temperature independent between  $115^\circ\text{C}$  and  $150^\circ\text{C}$ . In SmCP,  $\omega(T)$  can be described by an Arrhenius curve with activation energy  $E_A = 6.05\ \text{kJ/mol}$ . In SmX, the activation energy may be slightly higher, but the range is too narrow to obtain a reliable quantitative  $E_A$  there.

These experimental results can be summarized as follows: The angular frequency  $\omega$  is proportional to the wave number  $\pi/L$  of the ground mode, any dispersion is below our detection level. At constant  $L$ ,  $\omega$  changes by about  $15\%$  in the accessible temperature range, oscillations are faster at lower temperatures. There is no systematic  $\omega(r)$  dependence. Note that a solid string with tension  $T$  and specific mass  $\mu$  has a ground mode frequency proportional to  $\sqrt{T/\mu}$ . If, naively, we equate the filament tension to the product of cylinder circumference and surface tension,  $2\pi r\sigma$ , this would lead to an  $r^{-1/2}$  dependence of  $\omega$ , in contrast to the experiment. The damping time  $\tau$  is inversely proportional to the filament length. Its temperature dependence is negligible. There is a weak radius dependence of  $\tau$  (Fig. 4).

For a description of the dynamics, we employ a simple harmonic oscillator model. An equation of motion of the liquid filaments can be constructed from inertial, elastic, surface tension and friction terms that influence the dynamics of vibrations in absence of external forces. As a prerequisite, we recollect possible contributions, including typical solid state elastic properties that might arise from the internal layer structure. From the surface energy per length  $dx$  of a cylinder with radius  $r$  and surface tension  $\sigma$ ,  $dE_s = 2\pi r\sigma dx$ , one obtains a force per unit length in  $z$  direction  $f_s = 2\pi r\sigma z''$ , primes denote derivatives respective to  $x$ . The kinetic energy per length  $dx$  of a filament with mass density  $\rho$ ,  $dE_i = \frac{1}{2}\pi r^2\rho \dot{z}^2 dx$ , yields an inertial force per length  $f_i = \pi r^2\rho \ddot{z}$ .

Orientational elasticity arises from induced deformations of the director field. The magnitude of the related elastic energy per length is of the order of  $dE_{or} \approx \frac{1}{2}\pi r^2 K (z'')^2 dx$ , where a single effective elastic constant  $K$  is assumed for simplicity. Reasonable values of  $K$  are in the range of pN, and thus the related force term  $f_{or} \approx -\pi r^2 K z^{(iv)}$  can be neglected in comparison to the other forces. Form elasticity may contribute a term  $dE_e = \frac{1}{2}E (z'')^2 dI$ , with the geometrical moment of inertia per length of the cylinder  $dI$  and an elastic modulus  $E$ . One arrives at  $f_e = -\frac{\pi}{4}r^4 E z^{(iv)}$ .

Further, we consider viscous friction of the oscillating filament in air: The filament segment at the antinode of the deflection moves with a maximum velocity  $v_0 = \max(\dot{z})$ . Experimentally,  $v_0$  is of the order of  $0.3\ \text{m/s}$  or less. Using the kinematic viscosity of air at  $100^\circ\text{C}$ ,  $\nu_{\text{air}} \approx 2.3 \cdot 10^{-5}\ \text{m}^2/\text{s}$ , Reynolds number  $\text{Re}$  and drag coefficient  $c_D$  for a filament with  $r = 25\ \mu\text{m}$  are  $\text{Re} = 2vr/\nu_{\text{air}} \approx 0.64$ ,  $c_D = 8\pi/[\text{Re}(2.002 - \ln \text{Re})] \approx 16$ , respectively. The friction force per length is  $f_f = -c_D (A/d\ell) \rho_{\text{air}} v^2/2$ ,  $|f_f| \approx 16\nu_{\text{air}}\rho_{\text{air}}v = 16\eta_{\text{air}}v$ .

From the measured parameters, one can estimate amplitudes of these forces:  $\bar{f}_s \approx 400\ \mu\text{N/m}$ ,  $\bar{f}_i \approx 1750\ \mu\text{N/m}$ ,  $\bar{f}_f \approx 100\ \mu\text{N/m}$ ,  $\bar{f}_e \approx 30\ \text{E/MPa}\ \mu\text{N/m}$ . This estimation shows that friction in air should be very small, and form elasticity may become important

only if the unknown elastic modulus  $E$  is of the order of 10 MPa or higher. In addition to the terms defined above, we allow for some other possible terms in the dynamic equations: a hypothetical bulk force,  $f_\xi = \xi\pi r^2 z''$ , and a bulk friction force connected with shear in the filament,  $f_\nu = \pi r^2 \rho \nu z''$ , with the kinematic viscosity  $\nu$ . Further, we may have to consider local energy dissipation at the supports, which is independent of the filament length but may depend upon the radius  $r$ .

We write the equation of motion in the form

$$\ddot{z} + 2\gamma\dot{z} - \nu z'' - C^2 z'' + W^2 z^{(iv)} = 0, \quad (2)$$

related to the above defined parameters by

$$C^2 = \frac{2\sigma}{r\rho} + \frac{\xi}{\rho}, \quad W^2 = \frac{\pi}{4} r^4 E + \pi r^2 K, \quad (3)$$

and  $\gamma = 8\eta_{\text{air}}/(\pi r^2 \rho)$ . The ansatz  $z_\pm = z_0 \exp(\pm ikx + \sigma t)$  leads to  $\sigma^2 + 2\gamma\sigma + \nu k^2 \sigma + C^2 k^2 + W^2 k^4 = 0$  and one finds  $\sigma = -1/\tau \pm i\omega$  with

$$\frac{1}{\tau} = \frac{8\eta_{\text{air}}}{\pi r^2 \rho} + \frac{\nu k^2}{2}, \quad \omega = \sqrt{C^2 k^2 + W^2 k^4 - \frac{1}{\tau^2}}. \quad (4)$$

Boundary conditions are  $z(\pm L/2) = 0$ , and we take into account that in practice only the ground mode  $k = \pi/L$  is excited (Fig. 1, right). Two counterpropagating waves form the solution  $z(x, t) = z_0 \cos kx \cos \omega t \exp(-t/\tau)$ .

We can compare Eq. (4) with the experimental results obtained under isothermal conditions:  $\omega \propto k$  and  $1/\tau \propto k$  (Fig. 3). One finds that the  $W$ -term (contributions with  $z^{(iv)}$ ) is negligible. Both elastic terms,  $f_{\text{or}}$  and  $f_e$ , are too small to influence the filament dynamics, otherwise, the experimental dispersion relation  $\omega(k)$  would be nonlinear. Thus our interpretation essentially differs from that in [5]. The experimental  $1/\tau$  is one order of magnitude smaller than  $\omega$ . Hence we can approximate the  $\omega(k)$  dependence in Eq. (4) by  $\omega = Ck = (2\sigma/(r\rho) + \xi/\rho)^{0.5}k$ . Since the surface tension  $\sigma \approx 25$  mN/m has been measured in an independent experiment [4], and a density  $\rho = 10^3$  kg/m<sup>3</sup> may be assumed in good approximation, the pure surface tension related term  $\sqrt{2\sigma/\rho r}$  can be calculated. For a filament with 25  $\mu\text{m}$  radius, it yields 1.4 m/s, which is much too small to explain the experimental value 2.59 m/s from Fig. 3. Moreover, Fig. 4 shows that  $\omega$  has no systematic radius dependence. A dominant surface tension term would lead to  $\omega \propto \sqrt{r}$ .

The experimental filament length dependence of the damping rate yields  $1/\tau = 0.42$  m/s  $L^{-1}$ , i.e.  $\tau$  grows linearly with  $L$ . For  $L = 1.5$  mm, the measured damping rate is 360 ms<sup>-1</sup>. Damping by air, in contrast, should be independent of  $L$ , and it contributes less than 25 % to  $1/\tau$  in Eq. (4) (for  $r \approx 25$   $\mu\text{m}$ ). A bulk shear friction term would yield an  $L^2$  dependence of  $\tau$ . In order to explain the linear filament length dependence of  $\tau$ , one has to look for alternative dissipative effects (see below).

We have to conclude that the main contribution to the back-driving force is some bulk term,  $f_\xi$ , that depends on the second spatial derivative of  $z(x)$  and is proportional to the filament volume rather than to its surface. Surface tension related terms in the cylinder model are too small and yield a wrong  $\omega(r)$  dependence.  $\xi$  should be of the order of  $\approx 5$  kPa, its origin has to be explored yet. A static tension measurement reported in [4] seems to give

in approximation the classical surface energy  $E_s$ , but systematic measurements need to be performed. Otherwise, the forces contributing to  $\xi$  may be of dynamic origin, comparable with effects of a non-zero storage modulus of viscoelastic liquids. Measurements of the dynamic filament tension should clarify this point.

Before the electric field is switched off,  $z_0$  is given by the equilibrium of electric (Coulomb) forces and the leading time-independent term  $\rho C^2 z''$  in the equation of motion (2). Initial acceleration and deflection amplitude are connected by  $\ddot{z}(0,0) = C^2 z''(0,0)$ , this allows to estimate the amplitude of electric forces on the filament,  $f_{el} = \rho \ddot{z}(0,0) = \rho \omega^2 z_0$ , yielding  $\approx 600 \text{ kN/m}^3$  at  $E = 0.33 \text{ MV/m}$  (resp. charge density  $1.8 \text{ C/m}^3$ ).

The damping time  $\tau$  is proportional to the filament length  $L$ , and since at given deflection  $z_0$ , the initial kinetic/potential energy of the filament is proportional to  $L$ , the main contribution to energy dissipation should be independent of  $L$ . A reasonable explanation is that friction occurs only at the filament ends, where material floats into and out of the meniscus. Another consequence of  $\tau \propto L$  is that inside the filament, there is practically no dissipation. Weakly damped transversal waves of the filament are accompanied by friction-free plug flow along the filament axis and viscous friction at the filament menisci. Finally, we note that the same experiment performed with filaments in the  $B_7$  mesophase (of another mesogen) yields a qualitatively different picture: Instead of oscillations, a fast overdamped relaxation is observed. This is obviously due to an in-plane positional order of  $B_7$ , leading to strong internal dissipation.

This study was supported by the DFG with grant STA 425/15. H. Nádasi and W. Weissflog are gratefully acknowledged for the supply of mesogenic material.

## References

- [1] A.-G. Cheong, A.D. Rey, and P.T. Mather, Phys. Rev. E **64**, 041701 (2001)
- [2] D.H. Van Winkle and N.A. Clark, Phys. Rev. Lett. **48**, 1407 (1982)
- [3] F. Vollrath and D.P. Knight, Nature **410**, 541 (2001)
- [4] A. Eremin, A. Nemeş, R. Stannarius, M. Schulz, H. Nádasi, W. Weissflog, Phys. Rev. E **71** 031705 (2005)
- [5] A. Jákli, D. Krüerke, G.G. Nair, Phys. Rev. E **67**, 051702 (2003)
- [6] G. Pelzl, S. Diele, A. Jákli, C. Lischka, I. Wirth, and W. Weissflog, Liq. Cryst. **26**, 135 (1999)
- [7] D.R. Link et al., Science **278**, 1924 (1997)
- [8] A. Eremin, S. Diele, G. Pelzl, H. Nádasi, and W. Weissflog, Phys. Rev. E **67**, 021702 (2003)
- [9] R. Stannarius et al., Phys. Rev. E **65** 041707, (2002).
- [10] R. Stannarius and Ch. Cramer. Europhys. Lett. **42** 43, (1998).